

Selective and sensitive molecularly imprinted sol–gel film-based electrochemical sensor combining mercaptoacetic acid-modified PbS nanoparticles with Fe₃O₄@Au–multi-walled carbon nanotubes–chitosan

Yufang Hu · Zhaohui Zhang · Huabin Zhang ·
Lijuan Luo · Shouzhao Yao

Received: 11 December 2010 / Revised: 12 May 2011 / Accepted: 14 May 2011 / Published online: 1 June 2011
© Springer-Verlag 2011

Abstract A sensitive molecularly imprinted electrochemical sensor was developed for selective detection of streptomycin by combination of mercaptoacetic acid-modified PbS nanoparticles with Au-coated Fe₃O₄ magnetic nanoparticles dispersed multi-walled carbon nanotubes doped chitosan film. The imprinted sensor was fabricated onto the Au electrode via stepwise modification of nanocomposites and an electrodeposited thin film of molecularly imprinted polymers via sol–gel technology. The morphologies and electrochemical behaviors of the imprinted sensor were characterized by scanning electron microscope, cyclic voltammetry, and differential pulse voltammetry, respectively. The prepared sensor showed very high recognition ability and selectivity for streptomycin. Under optimal conditions, the imprinted sensor displayed good electrocatalytic activity to the redox of streptomycin. And the differential voltammetric anodic peak current was linear to the logarithm of streptomycin concentration in the range from 1.0×10^{-6} to 1.0×10^{-3} mol L⁻¹, and the detection limit obtained was 1.5×10^{-9} mol L⁻¹. This proposed imprinted sensor was used successfully for streptomycin determination in different injection solution samples.

Keywords Imprinted sensor · Fe₃O₄@Au nanoparticles · PbS nanoparticles · Multi-walled carbon nanotubes · Chitosan

Introduction

Recently, molecularly imprinted polymers (MIPs) [1–3], as a recognition element for sensors, have increasingly attracted considerable attention. Molecular imprinting involves positioning functional monomers around the template molecules by non-covalent interaction or reversible covalent interaction, followed by polymerization and the template removal. When a molecular “memory” within the imprinted polymer matrix is created, the target molecule could be selectively recognized according to the molecular “memory”. MIPs possess several advantages over their recognition element, including robustness and stability under harsh physical and chemical conditions, easiness of preparation, and the ability to “tailor” recognition material for target analytes that might lack a suitable recognition element. Therefore, inexpensive, robust, and reusable MIPs materials are potent alternatives for sensing materials [4, 5].

In addition to as a recognition material, the response signal is an indispensable part for chemical sensor. Namely, as a sensing material, diffusion of the analytes across the inorganic MIP film needs to be accelerated to obtain a quick response. Furthermore, to effectively convert the binding signals from the molecular recognition to detectable electrical signals, the proper design of the signal transducer still remains challenging to improve sensitivity of this sensing system. Recently, magnetic nanoparticles (NPs) [6, 7] have exhibited their advantages for their novel

Y. Hu · Z. Zhang · H. Zhang · L. Luo
College of Chemistry and Chemical Engineering,
Jishou University,
Hunan 416000, People's Republic of China

Z. Zhang (✉) · S. Yao
State Key Laboratory of Chemo/Biosensing and Chemometrics,
Hunan 410082, People's Republic of China
e-mail: zhaohuizhang77@163.com

properties. The magnetic NPs can be controllably separated from bulk systems by means of an external magnetic field. Among the magnetic materials, iron oxide nanoparticles have been extensively studied. However, the reactivity of iron oxide nanoparticles increases with the decrease in particle size, i.e., iron oxide NPs particles with relatively small sizes may undergo rapid degradation upon direct exposure to certain environments [8]. To avoid such problems, magnetic core–shell nanoparticles with Fe_3O_4 as the core and metal or metal oxide such as gold [9], silica [10], titania [11], and alumina [12] as the shell have been extensively proposed. Among them, Au as the shell has been considered as one of the best candidates for building novel magnetic core–Au shell NPs, which exhibits well intrinsic properties of the magnetic core and Au shell. Because of the good chemical compatibility, the magnetic core–Au shell NPs have been proven to be a simple, cheap, and effective way to construct electrochemical interfaces for catalysis and sensors [13].

Immobilizing nanoparticles composite materials to the transduction is also a key, which significantly affect the selectivity, sensitivity, stability, and response time of chemical sensor. In this paper, Fe_3O_4 @Au nanocomposite and multi-walled carbon nanotubes (MWNTs) were mixed with chitosan (CTS) to form a novel nanocomposite. Chitosan (CTS) is an abundant natural cationic biopolymer with excellent characteristics such as film-forming ability, biocompatibility, non-toxicity, good water permeability, and high mechanical strength and adhesion, which had been used in chemically modified electrodes [14, 15]. CTS has also been widely used in the electrochemical sensor, and Darder et al. created an electrochemical sensor using bidimensional nanostructured materials based on chitosan–clay nanocomposites [16]. Njagi et al. developed a sensitive electrochemical sensor based on chitosan and electro-polymerized Meldola blue for monitoring NO in brain slices [17]. Carbon nanotubes (CNTs) [18, 19] consisted of cylindrical graphite sheets with many unique electronic and mechanical properties, and CNTs have been widely used in the fields of electroanalysis including electrochemical sensor and electrocatalysis. Torabi et al. produced Fe–multi-walled carbon nanotubes (Fe–MWNTs) nanocomposite using electrochemical techniques onto platinum substrate [20]. Zheng et al. constructed a nitrite sensor using carbon nanotube/polyvanillin composite film as an electrocatalyst for the electrochemical oxidation of nitrite [21]. Jiang et al. investigated synthesis and electrochemical properties of single-walled carbon nanotube–gold nanoparticle composites [22].

In the present work, a novel electrochemical sensor based on an electrodeposited imprinted sol–gel thin film and the amplification of nanoparticles has been constructed for streptomycin determination. The MAA-modified PbS

NPs on the surface of Au electrode via self-assembly method served not only as a tool of amplification but also as a linker because of the special interaction between sulfhydryl groups with Au. Then the Fe_3O_4 @Au–MWNTs–CTS was initially assembled onto the surface of PbS NPs/Au electrode by applying a constant magnetic field and the abundant amino groups through chitosan. Due to the inherent specificity of MIPs and the sensing layer, the selectivity and sensitivity of the MIP/ Fe_3O_4 @Au–MWNTs–CTS/PbS NPs/Au electrode were investigated in detail and were tested in different injection solution samples successfully.

Experimental

Instruments and reagents

Electrochemical data were obtained with a three-electrode system using a CHI 660 electrochemical workstation (Shanghai Chenhua Apparatus Co.). The different prepared sensors were used as the working electrodes. A platinum wire and a saturated calomel electrode (SCE) were used as counter and reference electrodes, respectively. All potentials were relative to the reference electrode. The surface morphology of modified electrode was analyzed by a JSM-6700F scanning electron microscope (SEM).

All the chemicals were of analytical-reagent grade unless otherwise stated and used directly without further purification. Double-distilled water was used throughout this study. MWNTs with 20–30-nm diameters were obtained from Shenzhen Technology Co. Methyltrimethoxysilane (MTMOS, 97%), tetraethoxysilane (TEOS), and 3-aminopropyltriethoxysilane (98%, APTES) were provided by Sigma (USA). Streptomycin, oxacillin, benzylpenicillin, clindamycin, and erythromycin were obtained from Sigma (USA). Methacrylic acid (MAA) and HAuCl_4 were obtained from Sigma-Aldrich (Munich, Germany). $\text{FeCl}_3 \cdot 6\text{H}_2\text{O}$, $\text{FeCl}_2 \cdot 4\text{H}_2\text{O}$, chitosan (CTS), polyethylene glycol (PEG, MW400), and $\text{NH}_2\text{OH} \cdot \text{HCl}$ were purchased from Changsha Reagent Co. (Hunan, China). All chemical experiments were carried out in phosphate buffer solution (PBS, pH 7.0, 0.2 mol L^{-1}). The buffer solution was prepared by mixing potassium dihydrogen phosphate (KH_2PO_4) and potassium hydrogen phosphate (K_2HPO_4) (Guangdong Jieshan Chemical Plant, China), containing 10 mmol L^{-1} potassium ferricyanide ($\text{K}_3[\text{Fe}(\text{CN})_6]$)/potassium ferrocyanide ($\text{K}_4[\text{Fe}(\text{CN})_6]$) (1: 1).

Preparation of water-soluble PbS NPs

PbS NPs were prepared according to the literature [23]. Briefly, $2.0 \mu\text{L}$ MAA (99%) was added to 100 mL of

1 mmol L⁻¹ PbCl₂ solution under vigorous stirring, and the pH of the mixture was adjusted to ~11 with 0.5 mol L⁻¹ NaOH solution. After bubbled with N₂ for 30 min, 50 mL of 1.34 mmol L⁻¹ Na₂S solution was added dropwise to the solution. The reaction was carried out for 24 h under N₂ atmosphere, and a yellow colloid was formed gradually. The mixture was centrifuged for at least 30 min at 15,000 rpm to remove the supernatant, and the precipitate was washed and redispersed in 30 mL of water and stored at 4 °C.

Preparation of Fe₃O₄@Au–MWNTs–CTS nanocomposites

Fe₃O₄ nanoparticles were prepared by the chemical coprecipitation method with a slight modification [24]. Nitrogen gas was used in the whole process. FeCl₃·6H₂O (2.7 g) and FeCl₂·4H₂O (1.0 g) were ultrasonically dissolved in 100 mL of 1.2 mmol L⁻¹ aqueous HCl. Then 1.25 mol L⁻¹ aqueous NaOH (150 mL) was added under vigorous stirring, and a black precipitate formed immediately. After vigorous stirring for 30 min, the precipitate was magnetically separated and washed thoroughly with water until the supernatant liquor reached neutrality (pH ~7). The final precipitate was dispersed in 250 mL of water and then directly used to prepare Fe₃O₄@Au nanocomposites as follows.

Four milliliters of 4% HAuCl₄ was added dropwise to 250 mL of the Fe₃O₄ suspension under vigorous stirring, then 20 mL of 0.8 mol L⁻¹ NH₂OH·HCl was added, and the solution color immediately turned from black to deep red. After vigorous stirring for 30 min, another 4 mL of 4% HAuCl₄ was added to the mixture, followed by vigorous stirring for another 1 h. The yielded deep red precipitate was magnetically separated and washed with water four times to remove any non-magnetic particles, then it was dispersed into 25 mL of water and stored at 4 °C in a refrigerator. The final concentration of Fe₃O₄@Au was 26.7 mg mL⁻¹, as measured by vacuum drying a certain volume of Fe₃O₄@Au nanocomposites and weighing the product.

CTS-dispersed Fe₃O₄@Au–MWNTs were prepared by the method similar to that described by Yang et al. [25] and Jiang et al. [22]. In short, 0.5 wt.% of CTS solution was first prepared by dissolving CTS powder in 1% (v/v) acetic acid solution with stirring for 1 h at room temperature until completely dispersed. Then 1.0 mg of MWNTs (treated as the previous experiment and displayed in reference [26]) were added in 1.0 mL of above CTS solution and ultrasonicated for 2 h. The resultant black suspension appeared homogeneous and stable. Herein, Fe₃O₄@Au nanocomposite was added to the resultant MWNTs–CTS supernatant under vigorous stirring at room temperature for 30 min. The homogeneous mixture was then incubated at

80 °C for 1 h with stirring and the Fe₃O₄@Au–MWNTs–CTS nanocomposites were obtained.

Preparation of imprinted sol–gel solution

A total of 3.0 mL (13.5 mmol) of TEOS, 3.0 mL of ethoxyethanol, 3.3 mL (9.45 mmol) of PEG, 0.5 mL (2.7 mmol) of APTMS, 0.1 mL of HCl (0.1 mol L⁻¹), and 1.0 mL of H₂O were mixed and stirred to acquire a homogeneous original sol. Then, a total of 4.0 mL of this solution mixed with 0.5 mL 1.0 mmol L⁻¹ streptomycin solution was stirred for 2 h to obtain an imprinted sol–gel film, while the original solution (without streptomycin) was used for the preparation of non-imprinted reference sol–gel film.

Fabrication of the sensor

The schematic illustration of the procedure for preparation of the MIP/Fe₃O₄@Au–MWNTs–CTS/PbS NPs/Au electrode is shown in Fig. 1. Gold electrode was polished with 0.3 and 0.05 μm aluminum slurry to a mirror-like surface to remove adsorbed organic matter, and then sonicated in HNO₃, ethanol, and double-distilled water, respectively. After drying at room temperature, the clean gold electrode was immersed into water-soluble PbS NPs solution for 16 h to obtain the PbS NPs/Au electrode. The casting solution was allowed to dry at room temperature overnight. The modified electrode above was washed with water and then immersed in Fe₃O₄@Au–MWNTs–CTS nanocomposites solution for 24 h to prepare the Fe₃O₄@Au–MWNTs–CTS/PbS NPs/Au electrode. Finally, the resulting electrode was prepared with electrodepositing the imprinted sol–gel solution onto the Fe₃O₄@Au–MWNTs–CTS/PbS NPs/Au electrode by using cyclic voltammetry from –0.1 V to +1.0 V for 20 cycles at a scan rate of 50 mV s⁻¹ and left to dry overnight at room temperature. Thus, the MIP/Fe₃O₄@Au–MWNTs–CTS/PbS NPs/Au electrode and NIP/Fe₃O₄@Au–MWNTs–CTS/PbS NPs/Au electrode were obtained. The doped streptomycin was extracted from the imprinted film by repetitive immersion in PBS and then air-dried for 24 h.

Electrochemical detection

The electrochemical measurements were conducted in 10 mL of 10 mmol L⁻¹ K₃[Fe(CN)₆]/K₄[Fe(CN)₆] (1:1) PBS containing 1.0 mmol L⁻¹. Electrodeposition processes and layer-by-layer modification effect were observed to employ cyclic voltammetry (CV) from –0.1 V to +1.0 V with a scan rate of 50 mV s⁻¹. The extraction and washing step, selectivity, and sample analysis of the MIP/Fe₃O₄@Au–MWNTs–CTS/PbS NPs/Au electrode were

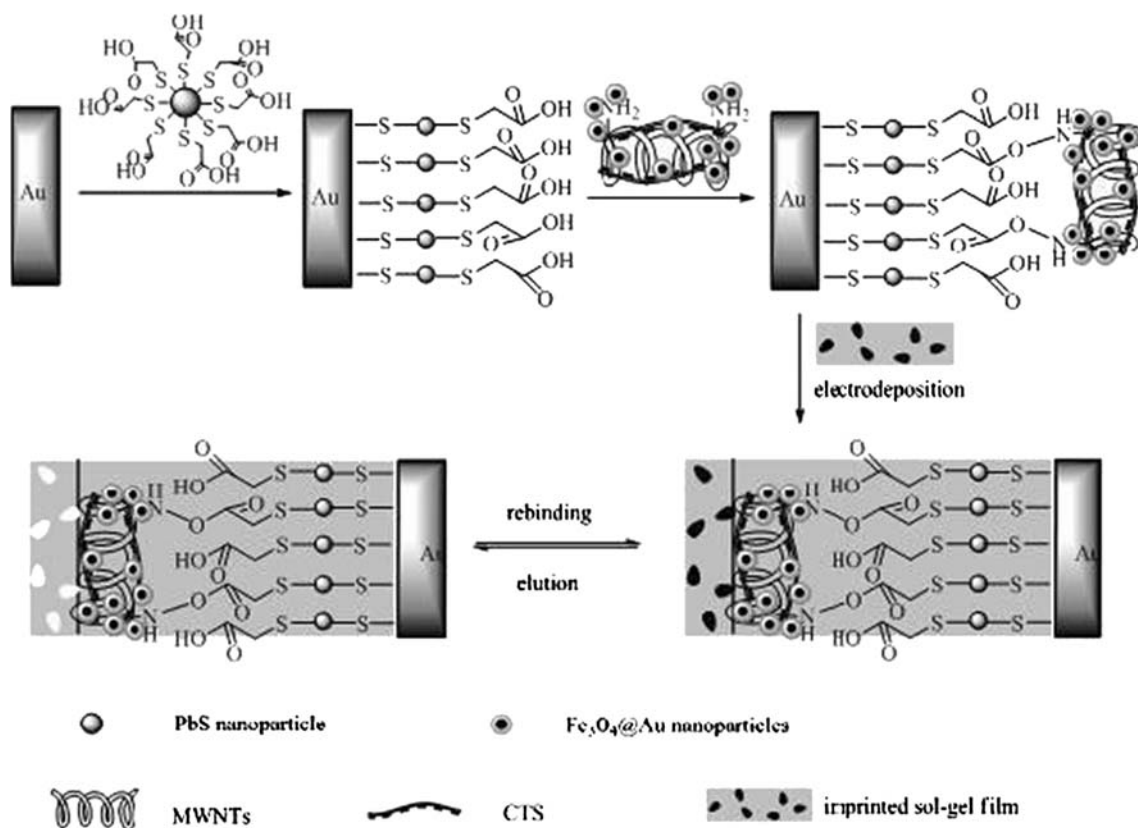


Fig. 1 Schematic illustration of the procedure for preparation of the MIP/ Fe_3O_4 @Au-MWNTs-CTS/PbS NPs/Au electrode

investigated by differential pulse voltammetry (DPV) from -0.2 V to $+0.6$ V, and parameters were performed as follows: the pulse amplitude was 50 mV, the pulse width was 50 ms, the pulse period was 200 ms, and the potential increment was 4 mV. All electrochemical experiments were carried out at room temperature.

Results and discussion

Electrodeposition process

The process of electrochemical deposition was carried out with cyclic voltammetry and the results are shown in Fig. 2. The response currents showed an increasing trend with the scanning cycles increased. When the scanning times increased from one to 20 cycles, the response current decreased obviously, which was caused by the insulation of imprinted sol-gel film, indicating the imprinted sol-gel film formed gradually. Thus, the peak current slightly decreases as further increasing scanning times over 20 cycles, even mostly coincident, which suggested that the imprinted film had been formed completely. The response current at the MIP/ Fe_3O_4 @Au-MWNTs-CTS/PbS NPs/Au electrode

(Fig. 2a) showed to be much higher than that at the MIP/Au electrode (Fig. 2b); this can be ascribed to the introduction of the nanocomposite material, thus effective area and active sites for electron transfer were enhanced.

Scanning electron microscopy (SEM) was performed to characterize the morphologies of the different modified electrodes, and the results are shown in Fig. 3. As shown in Fig. 3a, a slippery Au electrode surface with special Au image was observed. When the Au electrode was immersed with PbS NPs solution, the special Au image disappeared and PbS NPs were covered on the surface of Au electrode uniformly (Fig. 3b). Then, a Fe_3O_4 @Au-MWNTs was attached with the CTS solution to the surface of PbS NPs/Au electrode (Fig. 3c). It can be observed from Fig. 3d that a dense thin film was covered onto the surface of the Fe_3O_4 @Au-MWNTs-CTS/PbS NPs/Au electrode after the electrodeposition process. The presence of carbon nanotubes in the thin MIP film implied that the sensor was fabricated perfectly.

Electrochemistry characteristics of the sensor

CV is an effective and convenient technique for probing the feature of the modified electrode surface. Here, CV was

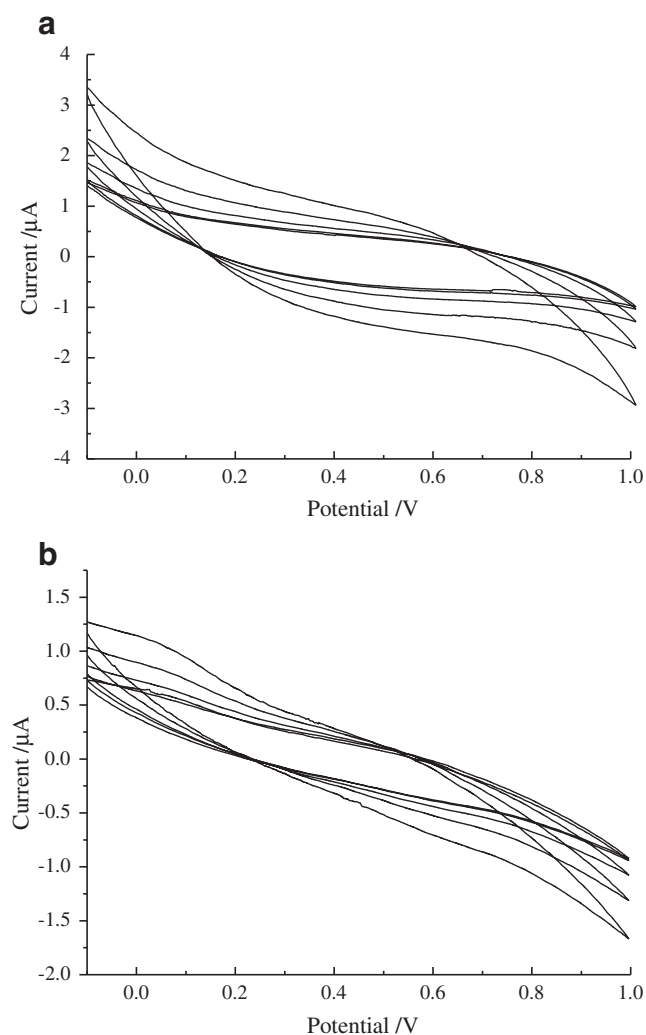


Fig. 2 Electrodeposition process of imprinted sol-gel solution at the **a** MIP/Fe₃O₄@Au-MWNTs-CTS/PbS NPs/Au electrode and **b** MIP/Au electrode; scanning cycles (from outer to inner): 1, 5, 10, 20, 30

used to investigate electrochemical behaviors after each assembly step. The CVs of the different modified electrodes in [Fe(CN)₆]^{3-/4-} solution are presented in Fig. 4. The redox-label Fe(CN)₆^{3-/4-} revealed a reversible CV at the bare Au electrode. After the pretreated Au electrode was modified with MAA-modified PbS NPs composite, the peak current increased greatly owing to MAA-modified PbS NPs layer could increase surface area and active sites for electron transfer. After MWNTs-CTS had been immobilized on the PbS NPs/Au electrode surface, the peak current increased clearly. This phenomenon may be ascribed to the presence of MWNTs-CTS, which severely enhanced effective area and active sites for electron transfer. Peak current increased in the same way after Fe₃O₄@Au was introduced the MWNTs-CTS layer, indicating that Fe₃O₄@Au can firmly enhance the electron

transfer between redox centers and electrode surfaces. When the imprinted sol-gel film was electrodeposited on the Fe₃O₄@Au-MWNTs-CTS/PbS NPs/Au electrode surface, a dramatic decrease in current was observed. This was attributed to the formation of imprinted sol-gel sensing layer, which acts as the inert electron and mass transfer blocking layer and it hinders the diffusion of ferricyanide toward the electrode surface. Furthermore, after electrodeposition of the non-imprinted sol-gel solution, the lowest peak current was observed owing to the absence of special binding sites and presence of non-special cavities. However, when the MIP electrode was incubated in 1.0 mmol L⁻¹ streptomycin and other interfering substances for 10 min, the highest apparent peak current in PBS containing streptomycin was exhibited compared with other reference substances, and the results are displayed in Fig. 4 (inset). The results suggested that the developed sensor showed good selectivity based on excellent sensitivity which can be enhanced to introduce nanocomposite materials, indicating that imprinted sol-gel film had been immobilized on the modified electrode surface.

Electrochemical responses to streptomycin and washing effect

In order to study the streptomycin recognition ability of MIP, the MIP film and NIP film electrodes were prepared and then immersed into the streptomycin-containing solutions. After 10 min, the electrodes were removed from the streptomycin solutions, and DPV was carried out. The obtained results are shown in Fig. 5. As can be seen, the DPV signal of the MIP film electrode (a, Fig. 5a) is higher than that of the NIP film (a, Fig. 5b). This indicates that the MIP film in the Au electrode intensively absorbs streptomycin from the aqueous solution in comparison to NIP film. In order to evaluate the streptomycin retention ability by MIP, after removing the electrodes from the streptomycin solution, they were inserted into the washing solution for different times. The obtained results are also displayed in Fig. 5. Washing the electrodes after streptomycin extraction does not considerably affect the streptomycin signal in the MIP film. After 10 s, the signal of MIP film reaches a steady state, and it seems that longer washing time does not noticeably decrease the MIP film signal. In comparison, the response of the NIP film electrode (curves b, c, and d in Fig. 5b) decreases to a large extent. Insets in Fig. 5 clearly confirm these statements. Hence, it is clear that the MIP film electrode has great affinity for streptomycin in comparison to NIP film. Thus, the enhancement of MIP film selectivity for streptomycin can be achieved by a simple washing step. The washing process can remove

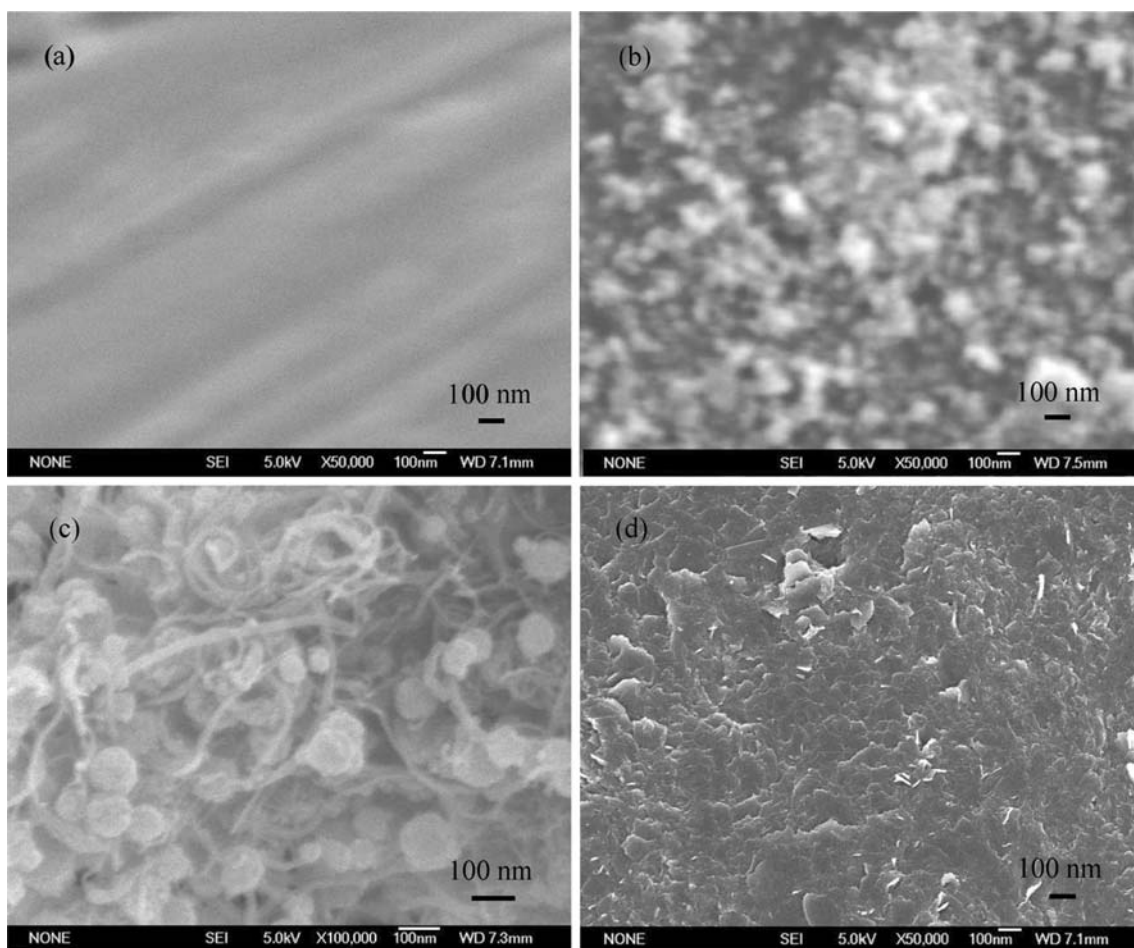


Fig. 3 SEM images of the different modified electrodes surface: **a** the bare Au electrode, **b** PbS NPs/Au electrode, **c** Fe_3O_4 @Au-MWNTs-CTS/PbS NPs/Au electrode, and **d** MIP/ Fe_3O_4 @Au-MWNTs-CTS/PbS NPs/Au electrode

weakly adsorbed and non-specifically adsorbed streptomycin molecules from the electrode surface, the state that is dominant in the case of NIP film electrode. However, streptomycin molecules that are incorporated in the MIP containing selective sites are not removed as easily by the washing process.

A major drawback of non-covalent systems is the unavoidable heterogeneity of the binding sites arising from the multitude of complexes formed between the template and the functional monomers. These are preserved to some extent during the polymerization. Usually, an excess of functional monomer relative to the template is required to favor template–functional monomer complex formation and to maintain its integrity during polymerization. As a result, a fraction of the functional monomers is randomly incorporated in the polymer matrix, resulting in the formation of non-selective binding sites. The cavities with incomplete or irregular shapes, as well as the non-selective binding sites, cannot absorb streptomycin molecules as tightly. The portion of streptomycin molecules absorbed by

the aforementioned binding sites can be removed from MIP film electrodes by the washing process. In the case of NIP film electrodes, the washing step easily removes the streptomycin from the electrode because the binding site in the NIP is non-selective and acts almost similarly to non-selective sites of MIP.

Effect of scan rate

Useful information involving electrochemical mechanism can usually be acquired from the relationship between peak current and scan rate. The CVs of the resulting sensor in PBS at different scan rates were investigated in the range of 10–1,000 mV s^{-1} . As shown in Fig. 6, the peak currents were dependent on the scan rate; current increased with the increase in scan rate. From the inset graph in Fig. 6, linear relationships with good correlation coefficients were observed between the peak current and the scan rate, suggesting that the electrochemical behavior was typical of a surface-controlled quasi-reversible process [27].

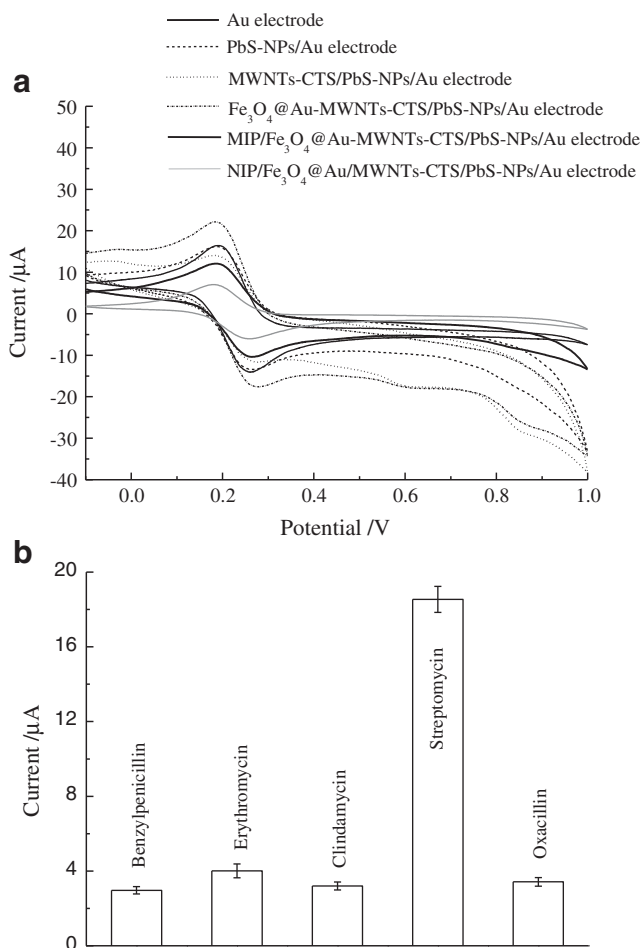


Fig. 4 **a** Cyclic voltammograms of the Au electrode, PbS NPs/Au electrode, MWNTs-CTS/PbS NPs/Au electrode, Fe₃O₄@Au-MWNTs-CTS/PbS NPs/Au electrode, MIP/Fe₃O₄@Au-MWNTs-CTS/PbS NPs/Au electrode, and NIP/Fe₃O₄@Au-MWNTs-CTS/PbS NPs/Au electrode in PBS. **b** Selectivity of MIP/Fe₃O₄@Au-MWNTs-CTS/PbS NPs/Au electrode

Optimization of the analytical conditions

Influence of the amount of APTMS and PEG on the response of the sensor

The effects of the amount of APTMS on the DPV responses of the MIP/Fe₃O₄@Au-MWNTs-CTS/PbS NPs/Au electrode are examined in Fig. 7a. With the molar ratio between APTMS and TEOS (APTMS/TEOS) increasing from 0.02 to 0.3, a peak current response was found at the ratio 0.2 for the MIP/Fe₃O₄@Au-MWNTs-CTS/PbS NPs/Au electrode (a, Fig. 7a), while the low current responses of the NIP/Fe₃O₄@Au-MWNTs-CTS/PbS NPs/Au electrode remained almost unchanged (b, Fig. 7a). Generally, APTMS acts as a functional monomer in the silica matrix providing hydrogen bond with the target molecule streptomycin. With its amount growing, more hydrogen bonds,

provided in the MIP film, will strengthen the interaction with streptomycin and leads to the increase in the current responses initially. However, when the ratio exceeded 0.2, the current of the MIP/Fe₃O₄@Au-MWNTs-CTS/PbS NPs/Au electrode decreased gradually. It is inferred that the structure of the film becomes denser and less porous with too much APTMS since the hydrolyzation and condensation rate of APTMS is much quicker than TEOS. Hence, the ratio 0.2 was chosen as the best for APTMS/TEOS.

On the other hand, the effect of the amount of PEG on the DPV responses of the MIP/Fe₃O₄@Au-MWNTs-CTS/PbS NPs/Au electrode is shown in Fig. 7b. Here, the signals were recorded on the MIP/Fe₃O₄@Au-MWNTs-CTS/PbS

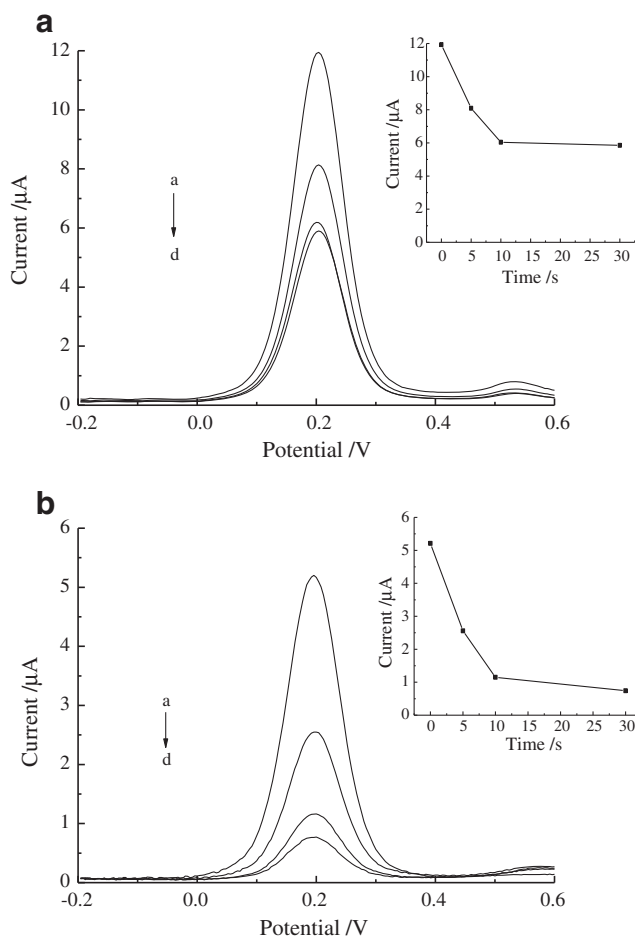


Fig. 5 Recorded streptomycin responses from the electrodes of **a** MIP/Fe₃O₄@Au-MWNTs-CTS/PbS NPs/Au electrode and **b** NIP/Fe₃O₄@Au-MWNTs-CTS/PbS NPs/Au electrode, after immersion into the streptomycin solution followed by electrochemical analysis (a) or washing and then electrochemical analysis (c-d). The insets of (a) and (b) show the effect of electrode washing repetitions on the related voltammetry responses of MIP/Fe₃O₄@Au-MWNTs-CTS/PbS NPs/Au electrode and NIP/Fe₃O₄@Au-MWNTs-CTS/PbS NPs/Au electrode, respectively, after removing the electrodes from streptomycin solution. Streptomycin extraction pH=7.0, extraction time=10 min, washing time=15 s

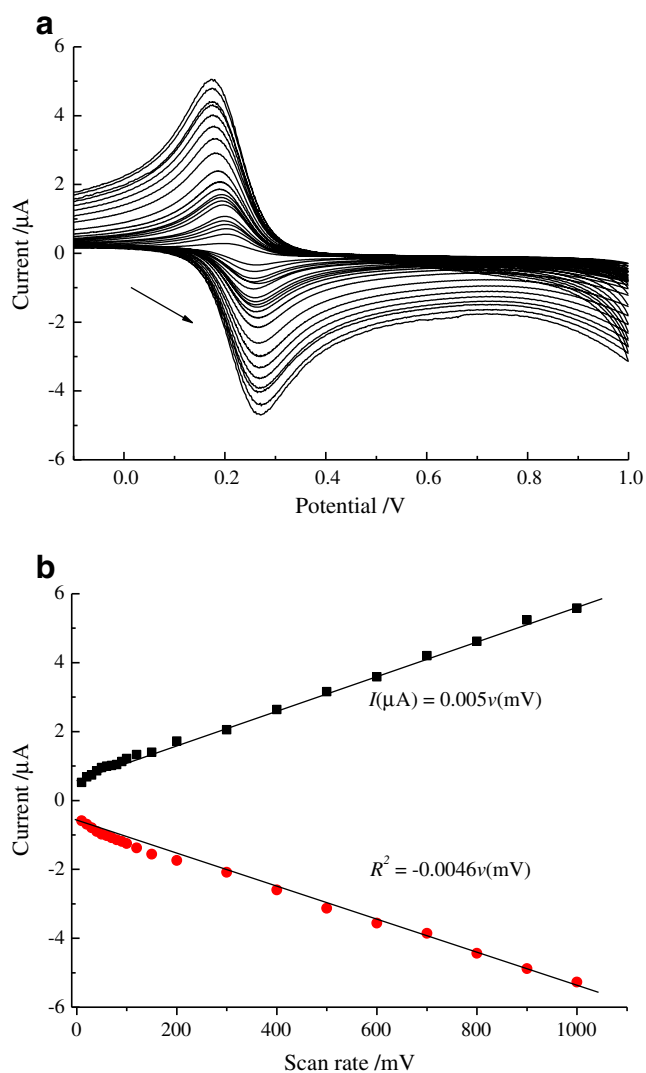


Fig. 6 **a** Cyclic voltammograms of the MIP/Fe₃O₄@Au-MWNTs-CTS/PbS NPs/Au electrode in PBS (pH 7.0) at scan rates of 10, 20, 30, 40, 50, 60, 70, 80, 90, 100, 120, 150, 200, 300, 400, 500, 600, 800, 900, and 1,000 mV s⁻¹ (from internal to external). **b** Plots of the peak currents vs. scan rate

NPs/Au electrode before the extraction of streptomycin. With the molar ratio between PEG and TEOS (PEG/TEOS) increasing from 0.1 to 1.0, the anodic peak current responses were found growing quickly at first and then increased slowly after the ratio 0.7. The presence of PEG makes the silica structure of the MIP film more porous and flexible; quick diffusion of the analyte streptomycin can be easily attained in such a film. Consequently, the current responses increased noticeably in the beginning. However, too much PEG will enhance the fluidity of the matrix and reduce the stability of the film, especially in aqueous solution [28]. It caused the slow growth of the currents from 0.7 to 1.0. Hence, the ratio of 0.7 was chosen as the best PEG/TEOS.

Effect of incubation time

In addition, the reaction conditions including incubation time affected the determination. The effect of incubation time on DPV peak current is shown in Fig. 8a. With the increase in the incubation time, the electrochemical response of the immobilized label increased and then reached a plateau at about 60 min. Therefore, to maximize the signal and minimize the assay time, 60 min was chosen as the optimal incubation time.

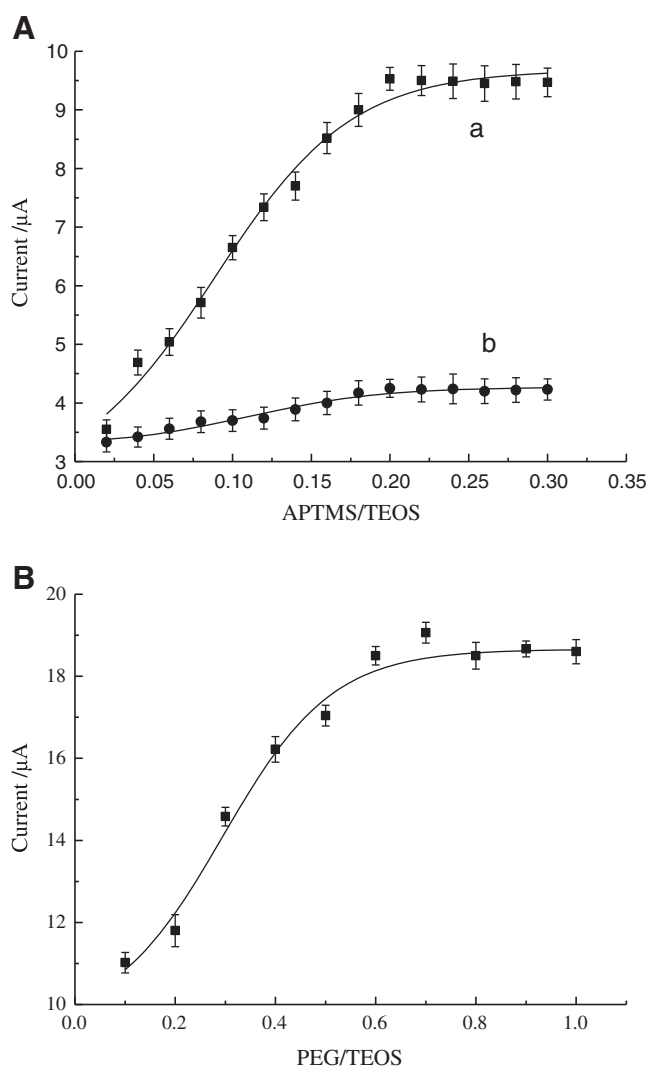


Fig. 7 **a** Influence of the ratio APTMS/TEOS on the anodic peak current of (a) MIP/Fe₃O₄@Au-MWNTs-CTS/PbS NPs/Au electrode and (b) NIP/Fe₃O₄@Au-MWNTs-CTS/PbS NPs/Au electrode. The electrodes were incubated in 1.0 mmol L⁻¹ streptomycin for 10 min. **b** Influence of the ratio PEG/TEOS on the anodic peak current of the MIP/Fe₃O₄@Au-MWNTs-CTS/PbS NPs/Au electrode before extraction ($n=3$)

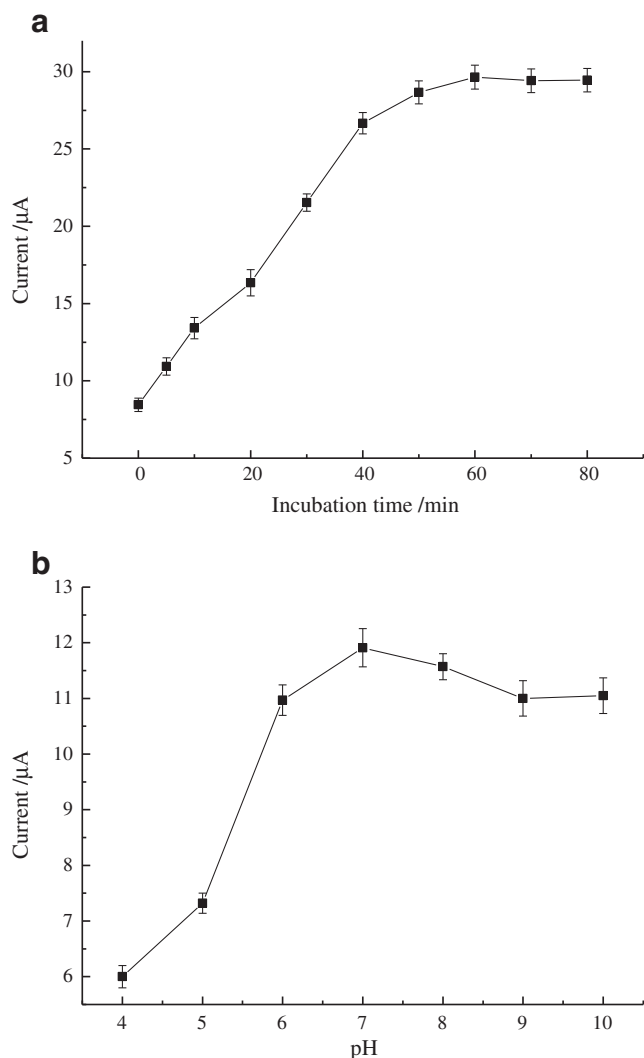


Fig. 8 Effects of **a** incubation time and **b** pH of detection solution on peak currents of DPV for 1.0 mmol L⁻¹ ($n=3$)

Influence of pH

The acidity of the solution greatly affected the electrochemical behavior of the sensor. Figure 8b shows the effect of pH of the electrolyte on the current of the determination over a pH range from 5.0 to 10.0 at 1.0 mmol L⁻¹. The results indicated that the excellent pH range was between 6.0 and 8.0. With a lower pH or a higher pH value, the weakened chelate effect will make the signal decrease. So pH 7.0 PBS was selected for detection.

Calibration curve and interference

Under the optimal analytical conditions, the determination of streptomycin with different concentrations was performed. The anodic peak current was linear to the logarithm

of the concentration of streptomycin from 1.0×10^{-6} to 1.0×10^{-3} mol L⁻¹ (Fig. 9). The linear regression equation was expressed as $i_p = 17.565 + 2.638 \log C$ [i_p (μA), C (mol L⁻¹), $r=0.993$] and the detection limit was estimated to be 1.5×10^{-9} mol L⁻¹. For eight parallel measurements of the MIP/Fe₃O₄@Au/MWNTs-CTS/PbS NPs/Au electrode incubated in PBS containing 1.0 mmol L⁻¹ streptomycin, the RSD of peak current was calculated to be 3.6%. The DPV response of the MIP/Fe₃O₄@Au-MWNTs-CTS/PbS NPs/Au electrode was also investigated within a week, during which the peak current did not change noticeably. That indicates the satisfactory stability of the electrode, which could be ascribed to the rigid structure of the MIP film.

The influence of foreign compounds was also tested by the MIP/Fe₃O₄@Au-MWNTs-CTS/PbS NPs/Au electrode. Benzylpenicillin, clindamycin, oxacillin, and erythromycin (their structures are shown in Table 1), another anti-inflammatory drug widely used in clinical treatment of inflammation, are analogues of streptomycin. When the electrode was incubated in 1.0 mmol L⁻¹ different analogues for 1 h, the peak current was just commensurate with the response produce by 0.1 mmol L⁻¹ streptomycin. It was also found that several kinds of surfactants such as Tween-20, Triton X-100, and sodium dodecyl sulfate did not interfere. Furthermore, 100-fold vitamin C, antipyrine, norfloxacin, allopurinol, thiamine, glucose, phenylalanine, captopril, or hydroxyzine had no obvious effect on the determination. Therefore, satisfactory selectivity of streptomycin was obtained by such a kind of sensor.

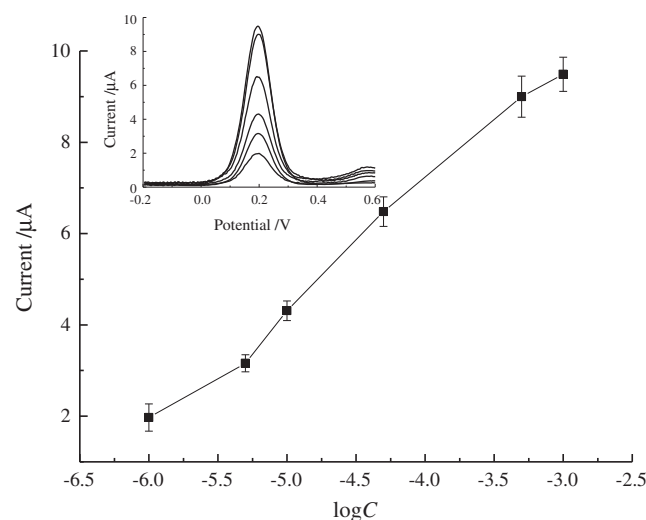
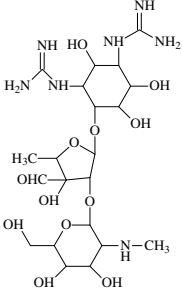
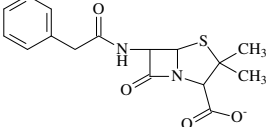
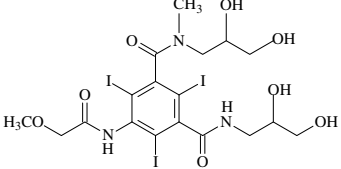
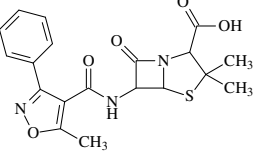
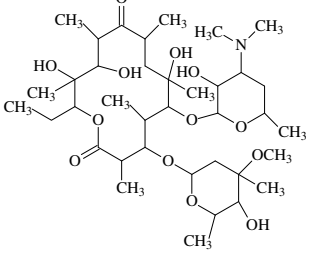


Fig. 9 Dependence of anodic peak current on logarithm of streptomycin concentration on the MIP/Fe₃O₄@Au-MWNTs-CTS/PbS NPs/Au electrode. The inset shows the DPV responses of 1.0×10^{-6} , 5.0×10^{-6} , 1.0×10^{-5} , 5.0×10^{-5} , 5.0×10^{-4} , and 1.0×10^{-3} mol L⁻¹ streptomycin (from bottom to top) after 10 min of incubation ($n=3$)

Table 1 Chemical structure of the used molecules

| Analyte | Structure |
|------------------|--|
| Streptomycin |  |
| Benzylpenicillin |  |
| Clindamycin |  |
| Oxacillin |  |
| Erythromycin |  |

Applications

To evaluate the feasibility of the new sensing system for possible clinical applications, the sensor was used for determining the recoveries of five different concentrations of streptomycin injection solution. The experimental results are shown in Table 2 and the recovery was in the range of 92–102%, which indicated that the developed sensor might be preliminarily applied for the determination of streptomycin in human serum for routine clinical diagnosis.

Table 2 Determination and recovery results of streptomycin in different injection solutions

| Sample number | Standard value (ng mL ⁻¹) | Determined value (ng mL ⁻¹) | Recovery ^a (%) |
|---------------|---------------------------------------|---|---------------------------|
| 1 | 5 | 4.6 | 92.0 |
| 2 | 10 | 10.2 | 102.0 |
| 3 | 15 | 14.7 | 98.0 |
| 4 | 20 | 20.1 | 100.5 |
| 5 | 30 | 29.8 | 99.3 |

^a Average of three experiment results

Conclusions

A sensitive and selective electrochemical sensor was fabricated for the detection of the streptomycin via stepwise modification of MAA-modified PbS NPs, Fe₃O₄@Au–MWNTs–CTS, and a thin MIP film on Au electrode surface. The excellent performance of the MIP/Fe₃O₄@Au–MWNTs–CTS/PbS NPs/Au electrode towards streptomycin can be ascribed to the Fe₃O₄@Au–MWNTs–CTS/PbS NPs functional monolayer with electrochemical catalytic activities and the porous MIP film with plentiful selective binding sites. Under the selected analytical conditions, the anodic peak current was linear to the logarithm of streptomycin concentration from 1.0×10^{-6} to 1.0×10^{-3} mol L⁻¹ with the detection limit of 1.5×10^{-9} mol L⁻¹. The Fe₃O₄@Au–MWNTs–CTS/PbS NPs functionalized MIP sensor, with high selectivity, sensitivity, and speed, meets the requirements of streptomycin detection, and it could be potentially applied in clinical analysis of physiological samples.

Acknowledgments This work has been co-supported by the Nature Science Foundation China (No. 21005030), the Colonel-level Project of Jishou University of Hunan Province, China (No. 09JDY007), and the Graduate Innovation Foundation of Hunan Province, China (No. CX2010B294).

References

- Liang RN, Zhang RM, Qin W (2009) Potentiometric sensor based on molecularly imprinted polymer for determination of melamine in milk. *Sens Actuators B* 141:544–550
- Blanco-López MC, Lobo-Castañón MJ, Miranda-Ordieres AJ, Tuñón-Blanco P (2003) Voltammetric sensor for vanillylmandelic acid based on molecularly imprinted polymer-modified electrodes. *Biosens Bioelectron* 18:353–362
- Wu N, Feng L, Tan YY, Hu JM (2009) An optical reflected device using a molecularly imprinted polymer film sensor. *Anal Chim Acta* 653:103–108
- Blanco-López MC, Lobo-Castañón MJ, Miranda-Ordieres AJ, Tuñón-Blanco P (2004) Electrochemical sensors based on molecularly imprinted polymers. *Trends Anal Chem* 23:36–48
- Hillberg AL, Brain KR, Allender CJ (2005) Molecular imprinted polymer sensors: implications for therapeutics. *Adv Drug Deliv Rev* 57:1875–1889
- Wang SF, Xie F, Hu RF (2007) Carbon-coated nickel magnetic nanoparticles modified electrodes as a sensor for determination of acetaminophen. *Sens Actuators B* 123:495–500
- Thilwind RE, Megens M, Zon JBAD, Coehoorn R, Prins MWJ (2008) Measurement of the concentration of magnetic nanoparticles in a fluid using a giant magnetoresistance sensor with a trench. *J Magn Magn Mater* 320:486–489
- Salgueirino-Maceira V, Correa-Duarte MA, Spasova M, Liz-Marzán LM, Farle M (2006) Composite silica spheres with magnetic and luminescent functionalities. *Adv Funct Mater* 16:509–514
- Xu ZC, Hou YL, Sun SH (2007) Magnetic core/shell Fe₃O₄/Au and Fe₃O₄/Au/Ag nanoparticles with tunable plasmonic properties. *J Am Chem Soc* 129:8698–8699
- Deng YH, Qi D, Deng CH, Zhang XM, Zhao DY (2008) Superparamagnetic high-magnetization microspheres with an Fe₃O₄@SiO₂ core and perpendicularly aligned mesoporous SiO₂ shell for removal of microcystins. *J Am Chem Soc* 130:28–29
- Chen CT, Chen YC (2005) Fe₃O₄/TiO₂ core/shell nanoparticles as affinity probes for the analysis of phosphopeptides using TiO₂ surface-assisted laser desorption/ionization mass spectrometry. *Anal Chem* 77:5912–5919
- Chen CT, Chen WY, Tsai PJ, Chien KY, Yu JS, Chen YC (2007) Rapid enrichment of phosphopeptides and phosphoproteins from complex samples using magnetic particles coated with alumina as the concentrating probes for MALDI MS analysis. *J Proteome Res* 6:316–325
- Qiu JD, Xiong M, Liang RP, Peng HP, Liu F (2009) Synthesis and characterization of ferrocene modified Fe₃O₄@Au magnetic nanoparticles and its application. *Biosens Bioelectron* 24:2649–2653
- Dutta PK, Tripathi S, Mehrotra GK, Dutta J (2009) Perspectives for chitosan based antimicrobial films in food applications. *Food Chem* 114:1173–1182
- Bhatnagar A, Sillanpää M (2009) Applications of chitin- and chitosan-derivatives for the detoxification of water and wastewater—a short review. *Adv Colloid Interface Sci* 152:26–38
- Darder M, Colilla M, Ruiz-Hitzky E (2005) Chitosan–clay nanocomposites: application as electrochemical sensors. *Appl Clay Sci* 28:199–208
- Njagi J, Erlichman JS, Aston JW, Leiter JC, Andreescu S (2010) A sensitive electrochemical sensor based on chitosan and electro-polymerized Meldola blue for monitoring NO in brain slices. *Sens Actuators B* 143:673–680
- MacKenzie K, Dunens O, Harris AT (2009) A review of carbon nanotube purification by microwave assisted acid digestion. *Sep Purif Technol* 66:209–222
- Justin J (2005) Gooding nanostructuring electrodes with carbon nanotubes: a review on electrochemistry and applications for sensing. *Electrochim Acta* 50:3049–3060
- Torabi M, Sadmezhaad SK (2010) Electrochemical synthesis of flake-like Fe/MWCNTs nanocomposite for hydrogen evolution reaction: effect of the CNTs on dendrite growth of iron and its electrocatalytic activity. *Curr Appl Phys* 10:72–76
- Zheng DY, Hu CG, Peng YF, Hu SS (2009) A carbon nanotube/polyvanillin composite film as an electrocatalyst for the electrochemical oxidation of nitrite and its application as a nitrite sensor. *Electrochim Acta* 54:4910–4915
- Jiang HJ, Zhao Y, Yang H, Akins DL (2009) Synthesis and electrochemical properties of single-walled carbon nanotube–gold nanoparticle composites. *Mater Chem Phys* 114:879–883
- Hu KC, Liu P, Ye SJ, Zhang SS (2009) Ultrasensitive electrochemical detection of DNA based on PbS nanoparticle tags and nanoporous gold electrode. *Biosens Bioelectron* 24:3113–3119
- Pang LL, Li JS, Jiang JH, Le Y, Shen GL, Yu RQ (2007) A novel detection method for DNA point mutation using QCM based on Fe₃O₄/Au core/shell nanoparticle and DNA ligase reaction. *Sens Actuators B* 127:311–316
- Yang H, Wang SC, Mercier P, Akins DL (2006) Diameter-selective dispersion of single-walled carbon nanotubes using a water-soluble, biocompatible polymer. *Chem Commun* (13):1425–1427
- Huang KJ, Niu DJ, Xie WZ, Wang W (2010) A disposable electrochemical immunosensor for carcinoembryonic antigen based on nano-Au/multi-walled carbon nanotubes–chitosans nanocomposite film modified glassy carbon electrode. *Anal Chim Acta* 659:102–108
- Xu J, Shang FJ, Luong JHT, Razeeb KM, Glennon JD (2010) Direct electrochemistry of horseradish peroxidase immobilized on a monolayer modified nanowire array electrode. *Biosens Bioelectron* 25:1313–1318
- Brown KR, Walter DG, Natan MJ (2000) Seeding of colloidal Au nanoparticle solutions. 2. Improved control of particle size and shape. *Chem Mater* 12:306–313